the FEBS Journal

Identification of calreticulin as a ligand of GABARAP by phage display screening of a peptide library

Jeannine Mohrlüder[1,2], Thomas Stangler[1,2], Yvonne Hoffmann[1,2], Katja Wiesehan[2], Anja Mataruga[3] and Dieter Willbold[1,2]

1 Institut für Physikalische Biologie, Heinrich-Heine-Universität Düsseldorf, Germany
2 Institut für Neurowissenschaften und Biophysik (INB-2), Molekulare Biophysik, Forschungszentrum Jülich, Germany
3 Institut für Neurowissenschaften und Biophysik (INB-1), Zelluläre Biophysik, Forschungszentrum Jülich, Germany

Keywords
calreticulin; $GABA_A$ receptor; GABARAP; phage display screening; protein–protein interaction

Correspondence
T. Stangler or D. Willbold, INB-2 Molekulare Biophysik, Forschungszentrum Jülich, 52425 Jülich, Germany
Fax: +49 2461 61 8766
Tel: +49 2461 61 2100
E-mail: stangler@biophys.uni-duesseldorf.de or d.willbold@fz-juelich.de

(Received 29 June 2007, revised 30 July 2007, accepted 29 August 2007)

doi:10.1111/j.1742-4658.2007.06073.x

4-Aminobutyrate type A ($GABA_A$) receptor-associated protein (GABARAP) is a ubiquitin-like modifier implicated in the intracellular trafficking of $GABA_A$ receptors, and belongs to a family of proteins involved in intracellular vesicular transport processes, such as autophagy and intra-Golgi transport. In this article, it is demonstrated that calreticulin is a high affinity ligand of GABARAP. Calreticulin, although best known for its functions as a Ca^{2+}-dependent chaperone and a Ca^{2+}-buffering protein in the endoplasmic reticulum, is also localized to the cytosol and exerts a variety of extra-endoplasmic reticulum functions. By phage display screening of a randomized peptide library, peptides that specifically bind GABARAP were identified. Their amino acid sequences allowed us to identify calreticulin as a potential GABARAP binding protein. GABARAP binding to calreticulin was confirmed by pull-down experiments with brain lysate and colocalization studies in N2a cells. Calreticulin and GABARAP interact with a dissociation constant $K_d = 64$ nM and a mean lifetime of the complex of 20 min. Thus, the interaction between GABARAP and calreticulin is the strongest so far reported for each protein.

The control of neurotransmitter receptor expression and delivery to the postsynaptic membrane is of critical importance for neural signal transduction at synapses. The sorting, targeting and degradation of neurotransmitter receptors require mechanisms to regulate intracellular vesicular protein transport. These dynamic processes play a key role in the construction and functional maintenance of synapses, and are one of the underlying mechanisms of synaptic plasticity. 4-Aminobutyrate type A ($GABA_A$) receptors mediate fast synaptic inhibition in the brain and are the principal GABA-gated ion channels [1]. Inhibitory neurotransmitter receptors are of particular pharmacological importance, and are targets for drugs used to treat mental disorders or to modulate sleep and mood.

The human $GABA_A$ receptor-associated protein (GABARAP) is a protein implicated in the trafficking of $GABA_A$ receptors to the plasma membrane [2,3].

Abbreviations
CaN, calcineurin; CNX, calnexin; CRT, calreticulin; DDX47, DEAD box polypeptide 47; ER, endoplasmic reticulum; $GABA_A$ receptor, 4-aminobutyrate type A receptor; GABARAP, $GABA_A$ receptor-associated protein; GRIP1, glutamate receptor-interacting protein 1; GST, glutathione *S*-transferase; Ins(1,4,5)P_3, inositol 1,4,5-triphosphate; HSQC, heteronuclear single quantum coherence; LC3, light chain 3; MAP1 LC3, microtubule-associated protein 1 light chain 3; N2a, NEURO-2a; NHS, *N*-hydroxysuccinimide; NSF, N-ethylmaleimide sensitive factor; NaCl/P_i, phosphate buffer pH 7.6; PRIP-1, phospholipase C-related inactive protein type 1; PSSM, position-specific scoring matrix; SPR, surface plasmon resonance; SUMO, small ubiquitin-like modifier; UBL, ubiquitin-like modifier; Ubq, ubiquitin; ULK1, unc-51-like kinase 1.

GABARAP is a 14 kDa protein, which was identified by its interaction with the γ2 subunit of $GABA_A$ receptors [4]. A functional effect of GABARAP on the trafficking of $GABA_A$ receptors was demonstrated in neurones [5], and it was shown that GABARAP promotes GABA receptor clustering and modulates channel kinetics and conductance [6,7]. GABARAP is a ubiquitin (Ubq)-like modifier (UBL) and is enzymatically coupled to a target moiety in a Ubq-like manner [8]. By contrast with Ubq, GABARAP is not coupled to protein moieties, but forms a conjugate with phosphatidylethanolamine or phosphatidylserine [9], which is a unique feature of GABARAP and the homologous proteins of the light chain 3 (LC3)-like protein family. The microtubule-associated protein 1 light chain 3 (MAP1 LC3) family encompasses seven proteins with sequence identities to GABARAP ranging between 30% and 87%, which are implicated in autophagy and a variety of other vesicular transport processes. In addition to the γ2 subunit of $GABA_A$ receptors, a large variety of interaction partners, such as *N*-ethyl maleimide sensitive factor (NSF) [10], tubulin [4], unc-51-like kinase 1 (ULK1) [11], transferrin receptor [12], phospholipase C-related inactive protein type 1 (PRIP-1) [13], glutamate receptor-interacting protein 1 (GRIP1) [14], gephyrin [15] and DEAD box polypeptide 47 (DDX47) [16], have been reported to interact with GABARAP. Most interactions of GABARAP have not yet been characterized quantitatively. For some interactions, deletion constructs of GABARAP have been used to delineate the binding region. However, precise data on the binding site and mechanism of interaction, and structural data on a high affinity interaction, are not yet available.

Our aim was to identify GABARAP binding peptides from a phage displayed library of randomized peptides, in order to derive a sequence motif that could be used to search protein sequence data for novel GABARAP interaction partners. Calreticulin (CRT) was successfully identified as a novel GABARAP binding protein.

Results

In vitro selection of GABARAP peptide ligands

To determine the peptide binding specificity of GABARAP, recombinant glutathione *S*-transferase (GST)-GABARAP fusion protein was used to screen a phage displayed random dodecapeptide library. After four selection cycles, single clones were randomly chosen and assayed for GABARAP binding activity employing antiphage ELISAs to eliminate false positive clones.

```
-SHKSDWIFLPNA   N1
-SHKSDWIFLPNA
-SHKSDWIFLPNA
-GHLSDWVYVPMR
-GHLSDWVYVPMR
-GHLSDWVYVPMR
-GHLSDWVYVPMR
-GHLSDWVYVPMR
AHKSDNWVFLPE-
THINEKWVFLPQ-
VSMDDGWVFVQP-
VSMDDGWVFVQP-
VSMDDGWVFVQP-
VSMDDGWVFVQP-

 SLEDDWDFLPP    CRT(178-188)
```

Fig. 1. Multiple sequence alignment of phage display selected peptide sequences, which were selected against GABARAP and CRT(178–188). The conserved tryptophan residue is depicted in bold. The sequence of the N1 peptide is shown in the top line. The sequence fragment CRT(178–188) is shown in the bottom line.

Amino acid sequences of phage displayed peptides were deduced by DNA sequence analysis of 70 randomly chosen true positive clones. Some sequences were obtained multiple times; however, a single dominating peptide sequence was not observed. Three peptide sequences were chosen depending on their frequency of occurrence and intensity of the respective signal in the antiphage ELISA, and their binding affinity to GABARAP was determined (data not shown). The peptide with the sequence SHKSDWIFLPNAA was called 'N1' and was shown to bind the best. Figure 1 shows a sequence alignment of phage display selected peptides with highest similarity to N1.

Phage display selected peptide N1 binds to GABARAP

We quantitatively investigated the binding of fluorescein-labelled N1 peptide (fN1) to GABARAP by fluorescence titration experiments. Fluorescein fluorescence of fN1 was monitored in the presence of increasing amounts of GABARAP (Fig. 2). The fluorescence data obtained were fitted with a single site bimolecular ligand binding equation [17], resulting in an apparent K_d value of 0.74 ± 0.13 μM. Control experiments with fluorescein instead of fN1 did not result in saturable binding.

NMR investigations of unlabelled N1 binding to GABARAP labelled with the stable isotope ^{15}N (Fig. 3A) were in good agreement with the dissociation

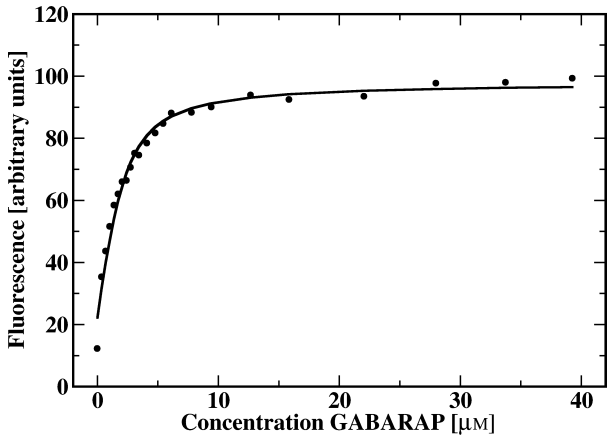

Fig. 2. Fluorescence titration of 2 μM of fluorescein-labelled N1 peptide with GABARAP. The fluorescence signal (●) is shown as a function of GABARAP concentration. Values result from the fluorescence of fluorescein-labelled N1 in the presence of the indicated concentration of GABARAP in comparison with a buffer control titration. Assuming a simple bimolecular interaction between fluorescein-labelled N1 peptide and GABARAP, the data were described by a model based solely on the law of mass action which accounts for ligand depletion. Nonlinear curve fitting of the model to the fluorescence data yielded a K_d value of 0.74 ± 0.13 μM (full line).

constant determined above. On addition of N1, many resonance signals of free GABARAP disappeared, and new signals, corresponding to peptide-liganded GABARAP, concomitantly appeared in the NMR spectrum. For some resonances, line broadening was observed. Hence, the GABARAP–N1 interaction occurs within intermediate to slow exchange on the NMR chemical shift difference timescale. This is indicative of low micromolar or submicromolar dissociation constants.

Identification of CRT as a potential GABARAP ligand

The phage display screening did not result in a single dominating peptide sequence. The considerable sequence diversity of our phage display selected peptides was used to our advantage by acknowledging that the selected peptide sequences together give a better description of GABARAP's peptide binding specificity than would the choice of a single peptide. In the multiple sequence alignment of the phage display selected peptides, a highly conserved tryptophan residue was observed. Defining this tryptophan residue as sequence position one (Trp +1), further sequence properties could be described. Obviously, aliphatic residues at positions 2 and 4, an aromatic residue at position 3 and a proline at position 5 or 6 seemed to support GABARAP binding. The positions N-terminally of Trp +1 displayed less sequence conservation. For positions −5 to −1, however, predominantly hydrophilic and charged amino acids were observed.

The set of phage display selected peptide sequences shown in Fig. 1 was used to create a representative consensus which accounted for the sequence variability within the set of peptides. A sequence position-specific scoring matrix (PSSM) was determined from the sequence alignment, which is depicted as a sequence logo in Fig. 4. The PSSM represents the amino acid tolerance and expected frequency at each position in a consensus block of related sequences, by contrast with the limited information available from each individual peptide. PSSM information was used to identify peptides that correspond to binding sites within the sequence of naturally occurring proteins. If a binding site in a protein–protein complex maps to a small peptide, it should be possible to identify this interaction by phage display and consensus determination, and to predict a potential *in vivo* protein–protein interaction.

For this purpose, a BLAST search of our PSSM against the Swiss-Prot protein database was used, and residues 178–188 of CRT were obtained as a sequence fragment with high similarity to our phage display derived motif. CRT(178–188) itself was not found in our phage display selected peptide sequences, but it aligns well with the multiple sequence alignment (Fig. 1), with the exception of position +2, which is a valine or isoleucine in the PSSM, and an aspartic acid (D184) in CRT.

Inspection of the putative binding site on a homology model of CRT (Fig. 5) showed that CRT(178–188) would be easily accessible for interaction with GABARAP.

Immunocytochemical localization studies in fixed NEURO-2a (N2a) cells showed that both proteins partially colocalize, or at least are not visibly separated, in different cellular compartments (Fig. 6). In addition to the reported cytosolic appearance of both GABARAP and CRT [4,18], these results indicate the possibility for direct interaction.

Recombinant GABARAP binds endogenous CRT

To investigate whether GABARAP binds native endogenous CRT, a pull-down assay was established using recombinant GABARAP immobilized on *N*-hydroxysuccinimide (NHS)-activated Sepharose (GABARAP-Sepharose). Proteins from rat brain extracts that bind to GABARAP-Sepharose were separated by SDS-PAGE and probed by western blot analysis for CRT immunoreactivity. Indeed, Sepharose-immobilized GABARAP was found to interact

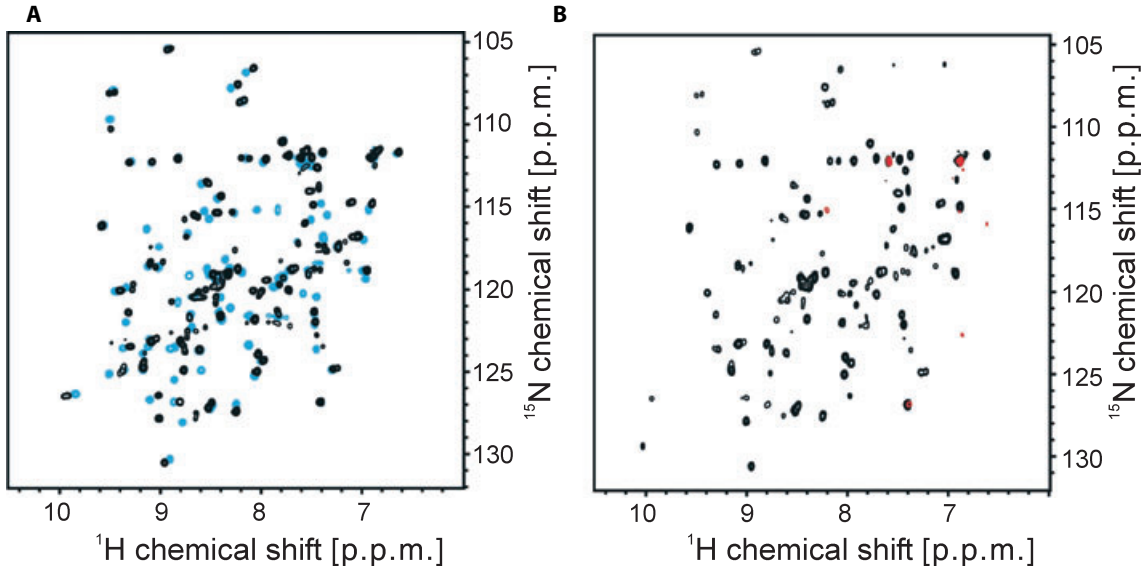

Fig. 3. ^{1}H–^{15}N HSQC spectra of GABARAP in the absence and presence of ligands. (A) Superimposed ^{1}H–^{15}N HSQC spectra of 190 μM GABARAP in the absence (blue contour lines) and presence (black contour lines) of 950 μM N1 peptide. During titration (data not shown), the blue-coloured peaks did not shift, but the signals broadened and their intensities decreased with ongoing titration, and new peaks (black) appeared. This indicates intermediate to slow exchange on the NMR chemical shift timescale, which is typical for a low micromolar or sub-micromolar dissociation constant. (B) ^{1}H–^{15}N HSQC spectrum of 20 μM GABARAP in the presence of 20 μM CRT (red contour lines) superimposed on a spectrum of 16 μM GABARAP in the presence of 16 μM CRT and 1180 μM N1 peptide (black contour lines). In the absence of N1 peptide, only very few resonances were observed. The signal threshold is set directly above the noise level. During titration (data not shown), new resonance signals (red) appeared. By comparison with the spectrum of N1-liganded GABARAP (A), these resonance signals can be attributed to N1-liganded GABARAP. By binding to GABARAP, N1 peptide displaces CRT from GABARAP. A few additional resonances with small line widths were observed. These resonances can be attributed to free N1 peptide because of the natural abundance of ^{15}N. Example resonances of the free N1 peptide are labelled (*), corresponding to the side chain amide group of Trp0 and C-terminal amidation of the peptide.

with endogenous CRT from brain extracts (Fig. 7A). By contrast, Sepharose without immobilized GABARAP, but otherwise identically treated, did not show CRT immunoreactivity.

Recombinant CRT binds endogenous GABARAP

The interaction of CRT and GABARAP was further confirmed by a pull-down experiment of endogenous GABARAP with recombinant CRT immobilized on NHS-activated Sepharose (CRT-Sepharose). CRT-Sepharose was exposed to rat brain extracts, and CRT-Sepharose-associated proteins were separated by SDS-PAGE and probed by western blot analysis for GABARAP immunoreactivity. Sepharose-immobilized CRT was found to interact with endogenous GABARAP from brain extracts (Fig. 7B). Obviously, the polyclonal anti-GABARAP serum did not react with one single protein moiety, but also with another, similarly, but not identically, sized protein. Pull-down of lipidated GABARAP would also result in an additionally detected protein band in SDS-PAGE [8,19].

GABARAP and CRT interact with high affinity

Surface plasmon resonance (SPR) is a rapid and sensitive method for evaluating affinities and real-time kinetics of molecular binding reactions [20]. SPR was used to investigate quantitatively the interaction of recombinant GABARAP with recombinant CRT. GABARAP was immobilized on a CM5 sensor chip using standard amine coupling procedures. The injection of CRT on the sensor chip resulted in binding to GABARAP, as indicated by an injection time-dependent increase in the SPR response. Dissociation of bound CRT from the sensor chip was very slow, indicating a very low dissociation rate of CRT from GABARAP. Apart from a small change in the bulk refractive index during injection, no interaction of CRT with the reference surface was observed. Each sensorgram could be quantitatively evaluated for kinetic parameters by a model for a single site bimolecular interaction.

Regeneration of the chip was very difficult. Harsh conditions, such as denaturating agents, led to a strong

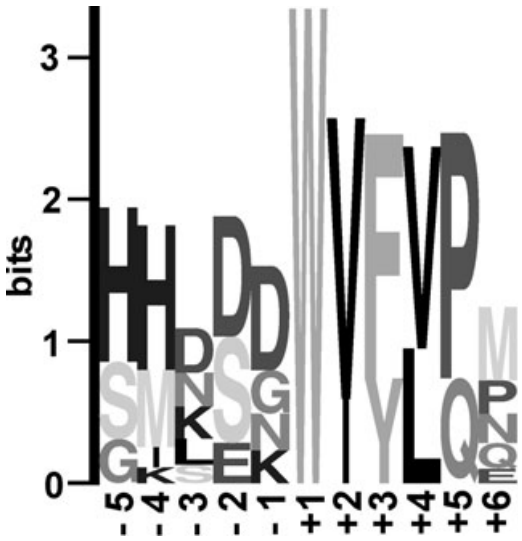

Fig. 4. A sequence logo illustrating the PSSM. The PSSM was derived from the multiple sequence alignment of phage display selected peptide sequences [59]. The positions are enumerated, respectively, to the central tryptophan residue Trp +1. A sequence logo is a graphical representation of aligned sequences where, at each position, the size of each residue is proportional to its frequency in that position, and the total height of all the residues in the position is proportional to the conservation of the position.

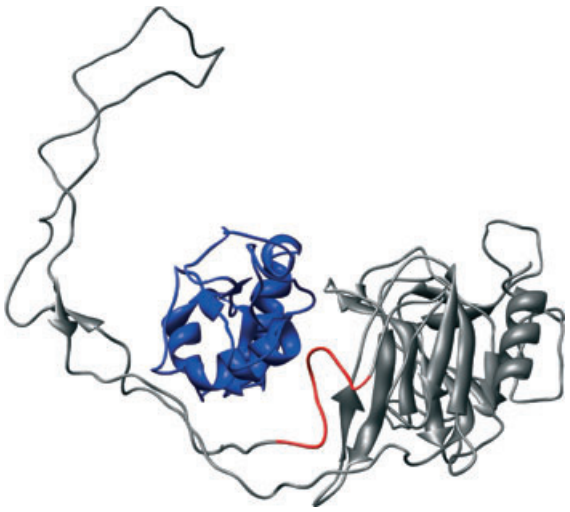

Fig. 5. Homology model of CRT(1–332) with an illustration of liganded GABARAP (PDB: 1kot). The homology model of CRT(1–332) (grey) was created using MODWEB [60] based on the crystal structure of calnexin (PDB: 1JHN). CRT(211–260) was manually replaced based on the solution structure of the P-loop (PDB: 1HHN). The globular and compact lectin-like domain encompassing the classical N-domain residues 1–170, as well as residues 286–332, is shown on the right side. The two-stranded hairpin-like fold, which forms an elongated arm-like shape protruding to the left from the N-domain, corresponds to the P-domain CRT(171–285). The linear binding site for GABARAP, CRT(178–188), is coloured red. For illustrative purposes, GABARAP is depicted in blue and has an arbitrary orientation close to its binding site on CRT. The molecular graphics image was produced using the UCSF CHIMERA package from the Resource for Biocomputing, Visualization, and Informatics at the University of California, San Francisco, CA, USA (supported by NIH P41 RR-01081) [61].

decrease in binding capacity. Mild conditions, e.g. high salt buffer, resulted in some regeneration, but still did not establish the pre-experiment conditions. After mild regeneration, an increased baseline and a decreased maximal binding capacity (R_{max}) were observed. This is clearly shown in Fig. 8, where two repeated injections of 1 μM and 100 nM of GABARAP exhibited different maximum binding values (R_{max}). However, quantitative analysis of the binding sensorgrams separately for each data set revealed the same binding kinetics for both binding events, but different maximum binding values (R_{max}). This suggests that the binding process is the same as before, although binding capacity has been lost, either during regeneration as a result of the partial denaturation of immobilized GABARAP, or because of the remaining CRT-occupied binding sites of immobilized GABARAP. The observation of decreasing binding capacity holds true for the whole series of successive binding experiments.

To extract binding kinetics, all binding curves were fitted simultaneously with a global association and global dissociation rate, but separate R_{max} values for each binding curve. The association rate k_{on} was determined to be 1.3×10^4 $M^{-1} \cdot s^{-1}$ and the dissociation rate k_{off} to be 8.3×10^{-4} s^{-1}. R_{max} values decreased, as expected, with increasing baseline. A dissociation constant of 64 nM for the GABARAP–CRT interaction was obtained. The overall fit of the experimental data can be considered to be very good, keeping in mind the potentially heterogeneous immobilization of GABARAP by amine coupling.

Further evidence for a direct high affinity interaction of recombinant and purified GABARAP and CRT in solution was obtained by NMR spectroscopy. NMR is very suitable for the study of the structure, dynamics and interactions of biological macromolecules [21]. ^{1}H–^{15}N correlation NMR (heteronuclear single quantum correlation, HSQC) spectra of GABARAP labelled with the stable isotope ^{15}N were recorded during the course of titration with unlabelled CRT. The NMR spectrum of GABARAP without CRT exhibited the known and expected resonances typical for natively folded GABARAP [22]. The addition of CRT to GABARAP resulted in the disappearance of GABARAP resonances, a clear indication of binding (Fig. 3B). Only weak amide signals for a Gln/Asn side chain and the C-terminal amino acid residue Leu117

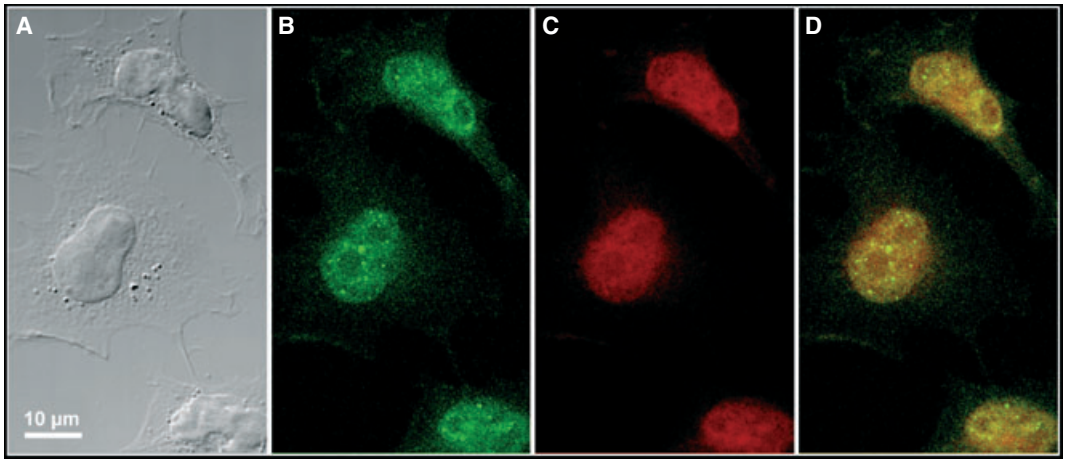

Fig. 6. Localization of GABARAP and CRT in fixed N2a cells. (A) Differential interference contrast image of N2a cells. (B) Immunofluorescence of Alexa488-labelled anti-GABARAP serum in green. (C) Immunofluorescence of Alexa647-labelled anti-CRT serum in red. (D) Merging of (B) and (C).

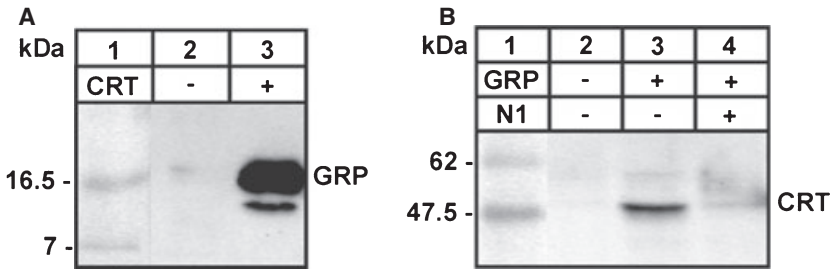

Fig. 7. GABARAP associates with CRT. (A) Endogenous CRT binds to immobilized GABARAP. Control Sepharose alone (lane 2) and Sepharose-coupled GABARAP in the presence (lane 3) and absence (lane 4) of 1150 µM N1 were exposed to rat brain extracts. After extensive washing, bound material was resolved by SDS-PAGE and analysed by immunoblotting with anti-CRT serum. Control Sepharose (lane 2) shows no indication for binding, whereas Sepharose-coupled GABARAP exhibits immunoreactivity for CRT. Only very weak immunoreactivity was observed in the presence of N1 peptide (lane 4). For convenience, lane 1 shows the bands of a prestained protein marker (Prestained Protein Marker, Broad Range, NEB, Beverly, MA, USA). (B) Endogenous GABARAP binds to immobilized CRT. Control Sepharose (lane 2) and Sepharose-coupled CRT were exposed to rat brain extracts. After extensive washing, bound material was resolved by SDS-PAGE and analysed by immunoblotting with anti-GABARAP serum. Two signals with GABARAP immunoreactivity are clearly visible.

were still observable, as a result of their higher degree of intrinsic flexibility within the CRT–GABARAP complex. However, under favourable conditions, the heterodimeric GABARAP–CRT complex would still be expected to give detectable NMR resonances of GABARAP in the CRT-bound state. The disappearance of GABARAP resonances indicates either a much larger size of the complex than expected or unfavourable dynamics in the complex. Oligomerization of CRT has been described in the literature [23,24]. Moreover, conformational exchange and line broadening were observed for the free CRT P-domain by NMR spectroscopy [25]. The disappearance of the GABARAP resonances could also result from conformational exchange phenomena for GABARAP in the CRT-bound state.

N1 peptide competes with CRT for GABARAP binding

CRT was identified as a putative GABARAP binding protein by a single linear sequence motif obtained from phage display selections. If this sequence motif is the primary determinant for CRT binding, the N1 peptide would be expected to compete for CRT binding to GABARAP. The competitive ability of the N1 peptide was investigated using CRT pull-down experiments (Fig. 7A). In the presence of a concentration of 1250 µM of peptide, CRT could not be pulled down from brain extract with immobilized GABARAP, indicating the ability of N1 peptide to competitively inhibit the binding of CRT to GABARAP.

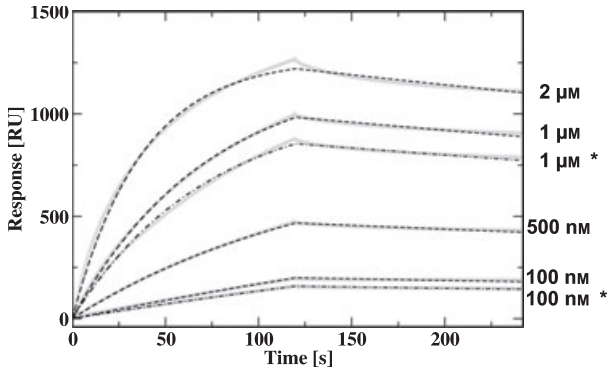

Fig. 8. Kinetic analysis of the interaction of CRT with immobilized GABARAP, as measured by SPR. Sensorgrams are shown in grey for various concentrations of CRT. They were recorded sequentially in the order 100 nM, 1 μM, 2 μM, 500 nM, 100 nM*, 1 μM*. Repeated concentrations exhibit decreased maximum binding and are designated in the figure (*). Data were recorded for a 120 s CRT association and a 120 s dissociation phase. The best fit to a single site bimolecular interaction model is shown in black. The association and dissociation rates, but not the maximum response R_{max}, were fitted globally, resulting in $k_{on} = 1.3 \times 10^4$ $M^{-1} \cdot s^{-1}$ and $k_{off} = 8.3 \times 10^{-4}$ s^{-1}.

A second competition experiment was performed using NMR spectroscopy and recombinant and purified proteins. ^{1}H–^{15}N HSQC NMR spectra of ^{15}N-labelled GABARAP were recorded during the addition of increasing amounts of N1 peptide to 20 μM GABARAP in the presence of 20 μM CRT. The addition of N1 resulted in the appearance of new and clearly observable resonances (Fig. 3B), although GABARAP was further diluted to 16 μM. Most new resonances were distinct from the resonances of free GABARAP, but were well dispersed and indicated stably folded GABARAP. The new resonances were at identical positions to the resonances of folded GABARAP in the N1-bound state (Fig. 3A). This clearly indicates a competitive displacement of CRT from GABARAP by the binding of N1 to GABARAP, suggesting the direct competition of the peptide with CRT for a common binding site on natively folded GABARAP.

Discussion

Phage display of a randomized peptide library is an effective and reliable screening assay to predict and characterize protein–peptide interactions [26]. In our phage display screen against GABARAP, a large variety of similar but not identical peptide sequences were observed. The observation that none of the phage display selected peptides clearly prevailed over others after four rounds of selection suggested that the peptides presumably interacted with GABARAP with similar affinities. This considerable sequence variability for GABARAP binding peptides suggests that GABARAP might be able to bind a variety of proteins containing nonidentical recognition peptide sequences. A representative peptide of the phage display screen, N1, interacted with GABARAP with a dissociation constant $K_d = 0.74$ μM, and exhibited predominantly slow exchange kinetics in NMR binding experiments. This affinity of GABARAP for N1 peptide was significantly stronger than for the peptides investigated by Knight *et al.* [27], who observed, in NMR-based investigations, exclusively fast exchange kinetics for a variety of peptides. This indicates a significantly increased dissociation rate, which, in turn, suggests a lower affinity of their peptides than the N1 peptide investigated here. Interestingly, one of the peptides investigated by Knight *et al.* [27] corresponds to a fragment of the γ2 subunit of the GABARAP receptor, γ2(394–411), which did not show any saturable binding for millimolar peptide concentrations. This very weak interaction contrasts with fluorescence binding studies [28], which suggest interaction with higher affinity. However, in our phage display screen, we did not find any peptide with similarity to $GABA_A$ receptor γ2 subunit peptide fragments.

A PSSM was constructed based on our phage display selected peptide sequences, acknowledging that the selected peptide sequences together give a better description of the peptide binding specificity of GABARAP than would the choice of a single peptide. CRT was identified as a high affinity interaction partner of GABARAP. CRT is a multifunctional, lectin-like 46 kDa protein best known as a luminal Ca^{2+}-dependent chaperone of the endoplasmic reticulum (ER) [29]. CRT is a regulator of ER Ca^{2+} homeostasis and is implicated in the regulation of Ca^{2+}-dependent signalling pathways. A large variety of physiological and pathological effects are associated with CRT, and it has also been implicated in processes which occur outside of the ER lumen [30,31]. CRT binds to a conserved sequence motif in the cytoplasmic domain of the α subunit of integrins [32], and has effects on cell adhesion [33]. It is a receptor for nuclear export [34] and modulates gene expression [35]. Retrotranslocation of CRT from the ER lumen to the cytosol has been reported recently [18], demonstrating that CRT can indeed change cellular compartments and that cytosolic CRT is derived from ER CRT. This retrotranslocation involves a pathway distinct from that used by unfolded proteins targeted for destruction [36].

Both GABARAP and CRT have received great attention in their respective fields. GABARAP is a

member of a protein family involved in vesicular transport phenomena, such as neurotransmitter receptor trafficking and autophagy. CRT, by contrast, is most recognized for its functions as a lectin-like Ca^{2+}-dependent chaperone of the ER. For both proteins, the interaction reported here is by far the strongest measured so far. The measured dissociation rate $k_{off} = 8.3 \times 10^{-4}\ s^{-1}$ corresponds to a highly stable complex between CRT and GABARAP with a mean lifetime of 20 min. Quantitative affinities of CRT–ligand interactions are known for ERp57 and glycans. Both interactions are related to the chaperone activity of CRT. The interaction of ERp57 with the CRT P-domain occurs with a K_d value between 9 and 18 μM and $k_{off} > 1000\ s^{-1}$, much weaker than that with GABARAP [37]. Glycans bind CRT with dissociation constants as low as 435 nM and $k_{off} = 0.1\ s^{-1}$ [38]. This is still significantly weaker than the observed affinity for GABARAP with CRT. CRT has also been shown to bind nonglycosylated peptides and unfolded or conformationally disturbed proteins [39,40]. The corresponding native proteins do not interact with CRT. By contrast with GABARAP, no quantitative data are available for these interactions. Most importantly, the interaction of CRT with GABARAP occurs with natively folded GABARAP. This is clearly indicated by the NMR spectra of free GABARAP and of N1-liganded GABARAP after displacement of CRT. Both spectra are typical of a folded protein, and no unfolded protein moiety was detected.

CRT(178–188) is proposed as the primary determinant of the GABARAP binding site of CRT, as this sequence is predicted by our phage display derived motif to interact with GABARAP. Moreover, the short N1 peptide with high similarity to CRT(178–188) interacts with GABARAP, with a dissociation constant $K_d = 0.74$ μM. The dissociation constant for the GABARAP–CRT interaction is, at $K_d = 64$ nM, significantly smaller. This could be the result of sequence differences between N1 peptide and CRT(178–188) or additional interactions beyond CRT(178–188), such as tertiary interactions.

Further evidence for CRT(178–188) as the primary binding site for GABARAP is provided by the displacement of CRT from GABARAP by N1 peptide. Although the possibility of an allosteric action of N1 on the GABARAP–CRT interaction cannot be strictly ruled out, our results suggest a competition of CRT and N1 for the same binding site on GABARAP.

Historically, the CRT sequence is subdivided into three sections: the N-domain, encompassing residues 1–170, the proline-rich P-domain, ranging from 171–285, and the highly acidic C-domain, ranging from 286–400. Despite great interest and efforts, no NMR or X-ray crystallographic high resolution structural data are available for full-length CRT. However, the structure of the CRT P-domain has been solved by NMR spectroscopy [25], and the structure of the homologous calnexin (CNX) ectodomain, corresponding to CRT(6–332), has been determined by X-ray crystallography [41]. Based on these data, CRT has a globular and compact lectin-like domain encompassing the classical N-domain residues 1–170 as well as residues 286–332. Inserted into the sequence of the globular domain is the P-domain, a two-stranded hairpin-like fold, which forms an elongated arm-like shape protruding from the N-domain. The binding motif for GABARAP is directly at the socket of the P-domain, in close vicinity to the globular domain of CRT (Fig. 5). The sequence segment of the binding motif is not contained in the investigated fragment of the NMR structure of the CRT P-domain. The sequence segment CNX(262–274), which poorly aligns with CRT(178–188) in a global sequence alignment, is not present in the crystal structure, as it could not be modelled with confidence into the electron density [41].

The CRT binding site of GABARAP is distinct from the known binding sites of CRT ligands. ERp57 interacts with the tip of the CRT P-domain [37]. The carbohydrate binding region is localized within the N-domain [41,42]. These interactions are of great importance for the ER functions of CRT; however, they are most probably irrelevant for cytosolic CRT. It is not yet known where potential cytosolic CRT-interacting proteins, such as integrins or glucocorticoid receptors, bind to CRT. Therefore, it remains to be investigated whether these interactions are of competitive or simultaneous nature to GABARAP binding. Moreover, it is not yet known where on GABARAP is the CRT binding site, and whether CRT competes with or allows for simultaneous interaction of GABARAP-interacting proteins, and thereby, most importantly, the interaction with the γ2 subunit of the $GABA_A$ receptor.

Experimental data on the effect of the GABARAP–CRT interaction on $GABA_A$ receptor transport and surface expression are not yet available; however, the strong interaction between GABARAP and CRT suggests a connection between CRT and $GABA_A$ receptor trafficking and localization. Indeed, both proteins interact with integrins, heterodimeric transmembrane proteins which mediate cell adhesion. Integrins are also important in synaptogenesis, as well as in the modulation of synaptic plasticity [43]. CRT copurifies with α3β1 integrin [44] and is an essential modulator of cell adhesion [33]. In addition, α3β1 integrin also colocalizes with $GABA_A$ receptors and affects GABAergic

eurotransmission [45]. CRT itself is also implicated in synaptic plasticity. Long-term sensitization training in *Aplysia* leads to an increase in CRT [46].

CRT has also been demonstrated to be involved in cytosolic inositol 1,4,5-triphosphate [Ins(1,4,5)P_3]-dependent Ca^{2+} signalling [47]. Moreover, the GABARAP binding protein PRIP-1 [13] is an Ins(1,4,5)P_3 binding protein. PRIP-1 is thought to protect Ins(1,4,5)P_3 against otherwise fast occurring hydrolysis, and is therefore involved in the regulation of Ins(1,4,5)P_3-mediated Ca^{2+} signalling [48]. Hence, GABARAP could implicate cytosolic CRT in PRIP-1-modulated Ins(1,4,5)P_3-induced Ca^{2+} signalling. The GABARAP-mediated implication of CRT in Ins(1,4,5)P_3-mediated cytosolic Ca^{2+} signalling, vesicular transport and synaptic plasticity is speculative. However, on the basis of these hypotheses, it will be possible to derive experimental strategies to investigate the physiological scope of the CRT–GABARAP interaction.

Probably the most obvious interpretation of the physiological role of the CRT–GABARAP interaction is associated with the Ubq-like properties of GABARAP. GABARAP is a UBL, like the small Ubq-like modifier (SUMO) or Ubq. UBLs are well known as sorting signals for trafficking events. SUMO, for example, alters the interaction properties of its targets, thereby often affecting their subcellular localization behaviour [49]. In the cell, GABARAP is indeed localized to membrane structures, such as transport vesicles, and allows for the recruiting of other factors which are necessary for correct vesicular transport. Such a factor could be cytosolic CRT. The purpose of this recruitment is not yet known, although we have outlined potential signalling pathways which might be affected by GABARAP-mediated CRT recruitment to transport vesicles. An important question to be answered is whether CRT interacts simultaneously or competitively with the variety of GABARAP-interacting proteins, e.g. the $GABA_A$ receptor PRIP-1 and the vesicular transport protein NSF. It is also worth mentioning that such a recruitment of CRT implicates a protein which is well known for its Ca^{2+} sensitivity in vesicular transport, and therefore a potential effector of Ca^{2+} signalling in GABARAP-mediated vesicular transport. CRT has a Ca^{2+} binding site with a K_d value of 1 μM [29], and is therefore amenable to regulation by physiologically relevant cytosolic free Ca^{2+} concentrations, which range between 0.1 and 10 μM. The Ca^{2+} dependence of CRT interactions with other ER proteins is well established [50]. Moreover, CRT can interact directly with the glucocorticoid receptor, and the CRT-mediated nuclear export of the glucocorticoid receptor is Ca^{2+} dependent [51].

The interaction of GABARAP with CRT opens up a new avenue for further experiments investigating the role of GABARAP in the cytosolic functions of CRT and, in addition, the role of CRT in the functions of GABARAP, such as the vesicular transport of $GABA_A$ receptors.

Experimental procedures

Phage display screening

A commercially available peptide library kit (PhD.-12 Peptide Library Kit, NEB, Beverly, MA, USA), containing 2.7×10^9 independent clones, was used to perform the biopanning as described in [17]. Recombinant GST–GABARAP fusion protein was used as bait. The progress of affinity selection was tracked by determining the GABARAP binding affinity of enriched sublibraries using an antiphage ELISA detection system. Before sequence analysis, single clones were randomly chosen after four rounds of selection and assayed for GABARAP binding activity employing antiphage ELISAs to eliminate false positive clones. Details about these antiphage ELISA systems have been described recently [17].

Motif extraction and database search

Our approach for motif extraction and database search followed closely that outlined previously [26]. Phage display selected peptide sequences were aligned with CLUSTALX using standard parameters [52]. Based on the alignment, a PSSM was constructed [53] using the BLOCKS multiple alignment processor tool (http://blocks.fhcrc.org/blocks/process_blocks.html). The PSSM was used in a BLAST search against the Swiss-Prot database employing the Motif Alignment & Search Tool MAST [54].

Peptides and proteins

Peptides were purchased as reversed phase high-performance liquid chromatography-purified products (JPT Peptide Technologies GmbH, Berlin, Germany). N1 peptide (H-SHKSDWIFLPNA-NH_2) was C-terminally amidated. fN1 peptide [H-SHKSDWIFLPNA-Lys(5,(6)carbofluorescein)-NH_2] was C-terminally fluoresceinylated. The cloning, expression and purification of GABARAP (Swiss-Prot accession number O95166) has been described previously [22]. At the outset, purchased CRT (Abcam, Cambridge, MA, USA) was used. Later, in-house-produced recombinant CRT was used. The CRT coding sequence was cloned into a modified pET15b vector (Novagen, Darmstadt, Germany). Sequence analysis of the resulting expression plasmid confirmed 100%

identity with human CRT (Swiss-Prot accession number P27797). CRT was expressed in *Escherichia coli* C43 (DE3) cells [55] and affinity purified using Ni^{2+}-nitrilotriacetic acid agarose beads (Qiagen, Hilden, Germany).

Immunocytochemistry

N2a cells were grown in 90% Dulbecco's modified Eagle's medium (DMEM) + 10% fetal bovine serum (FBS) + 0.005 mg·mL^{-1} gentamycin for 2 days on culture slides. N2a cells were fixed with 4% (v/v) formaldehyde in 100 mM phosphate buffer pH 7.6 (NaCl/P_i) and washed twice in 100 mM NaCl/P_i. Fixed cells were incubated for 15 min in NaCl/P_i, 5% ChemiBLOCKER (Chemicon/Millipore GmbH, Schwalbach, Germany) and 0.5% Triton X100, followed by 1 h of incubation of labelled antibody in NaCl/P_i, 5% ChemiBLOCKER and 0.5% Triton X100. The fixed cells were washed twice in NaCl/P_i. Nucleic acid staining was performed with Hoechst 33342 diluted in NaCl/P_i for 5 min, followed by two washing steps with NaCl/P_i. A cover slip was mounted on top of the cells using Aqua Poly Mount from Polysciences Europe GmbH (Eppelheim, Germany).

Antibody labelling was performed using antibody labelling kits from Invitrogen GmbH (Karlsruhe, Germany) (A30009, A20181) with the fluorophores Alexa488 and Alexa647. The antibodies used for labelling were as follows: CRT antibody PA3-900 (rabbit polyclonal, Affinity BioReagents, Golden, CO, USA) and rabbit polyclonal antibody generated against GABARAP. Both antibodies were purified using ProteinG-Sepharose prior to labelling. Cell culture slides were examined with a Leica TCS confocal laser scanning microscope (Leica Microsystems, Wetzlar, Germany) with a 63/1.32 oil immersion lens [56]. Contrast and brightness of the images were optimized in Adobe Photoshop. For double labelling, primary antibodies were mixed and applied simultaneously. The concentration of the antibodies, laser intensity and filter settings were carefully controlled, and the sequential scanning mode was employed to rule out completely cross-talk between the fluorescence detection channels. Bandpass filters of 500–530 nm for green fluorescence (Alexa488) and 680–750 nm for infrared fluorescence (Alexa647) were used.

Affinity purification 'pull-down' assays

Target protein (GABARAP or CRT) was coupled to NHS-activated Sepharose (NHS-activated Sepharose 4 Fast Flow, GE Healthcare, Uppsala, Sweden) according to the manufacturer's instructions. Extracts from rat brain lysate were exposed to Sepharose-coupled target protein. After extensive washing, the bound proteins were eluted with low pH buffer and subjected to SDS-PAGE. Proteins binding to the Sepharose-coupled target proteins or Sepharose alone were then detected by western blotting. The antibodies used were as follows: anti-CRT PA3-900 (rabbit polyclonal, Affinity BioReagents). Rabbit polyclonal antisera were generated against GABARAP and antigen purified. Blots were visualized using chemiluminescence (SuperSignal West Pico Chemiluminescent Substrate, Pierce, Rockford, IL, USA) and documented using a chemiluminescence detection system (ChemiDoc, Bio-Rad, Hercules, CA, USA).

Fluorescence titration

Fluorescence measurements were carried out at room temperature on a Perkin-Elmer (Rodgaue-Jügesheim, Germany) LS55 fluorescence spectrometer using excitation and emission wavelengths of 465 and 530 nm, respectively. GABARAP from a stock solution of 1.1 mM in 20 mM Hepes pH 7.2, 50 mM KCl and 5 mM $MgCl_2$ was added in small increments to 1 mL of 2 μM fluorescein-labelled N1 peptide (fN1) in the same buffer. On addition of protein solution, changes in fluorescence were measured. Dilution effects were corrected for by a control titration of fN1 with buffer only. The experimental data were described with a model of 1 : 1 binding solely based on the law of mass action accounting for ligand depletion [17]. Nonlinear curve fitting was carried out to fit the model to the experimental data and to obtain the dissociation constant K_d.

SPR

SPR studies were carried out on a Biacore X optical biosensor (Biacore, Uppsala, Sweden). Following Biacore's standard procedures for amine coupling, 1.5 μM of GABARAP protein in HBS-EP (10 mM Hepes pH 7.4, 150 mM NaCl, 3 mM EDTA, 1 mM β-mercaptoethanol, 0.05% surfactant P20) was used for the coupling of GABARAP to the carboxymethylated dextran matrix of a CM5 sensor chip surface. A reference surface was identically treated, but not subjected to GABARAP for immobilization. Experiments were performed in HBS-EP. Various concentrations of CRT were injected over the chip surface at 30 μL·min^{-1} and 21.5 °C to collect binding data. Biosensor data were prepared for analysis by subtracting the binding response observed from the reference surface from the response of the GABARAP-coupled surface.

Binding kinetics were determined by nonlinear least squares fitting of a model for single site bimolecular interaction to response data. The association and dissociation rates were fitted as global parameters, whereas the maximum response R_{max} was fitted as a separate parameter for each binding sensorgram. The dissociation constant was obtained as $K_d = k_{off}/k_{on}$.

NMR

All NMR spectra were recorded at 25 °C on a Varian (Darmstadt, Germany) Unity INOVA spectrometer at a

proton frequency of 600 MHz. The experiments for the GABARAP–N1 interaction were recorded with a Varian YZ-PFG-$^{1}H\{^{13}C,^{15}N\}$ probe. The sample contained 210 μM of GABARAP uniformly labelled with the stable isotope ^{15}N in 25 mM sodium phosphate pH 6.9, 100 mM KCl, 100 mM NaCl, 100 μM phenylmethanesulfonyl fluoride, 50 μM EDTA, 0.02% (w/v) sodium azide and 5% (v/v) deuterium oxide. The addition of N1 peptide resulted in a sample containing 190 μM GABARAP and 950 μM N1 peptide. ^{1}H-^{15}N HSQC spectra were collected with 96 complex points in the ^{15}N time domain, with eight scans per point in t1 and a 1 s recycle delay. The N1 competition experiment for the GABARAP–CRT interaction was recorded on a cryogenically cooled Varian Z-PFG-$^{1}H\{^{13}C,^{15}N\}$ probe. In order to be able to compete with CRT for GABARAP, low concentrations of GABARAP were used in this experiment. The sample contained 20 μM of GABARAP labelled with the stable isotope ^{15}N and 20 μM unlabelled CRT in the aforementioned NMR buffer with 5% (v/v) deuterium oxide. The addition of N1 peptide resulted in a sample containing 16 μM GABARAP, 16 μM CRT and 1180 μM N1 peptide. Competition experiment ^{1}H–^{15}N HSQC spectra were collected with 64 complex points in the ^{15}N time domain t1, with 256 scans per t1 point and a 1 s recycle delay. Data were processed with NMRPIPE [57] and analysed with CARA [58].

Acknowledgements

This work was supported by a Deutsche Forschungsgemeinschaft (DFG) grant to DW (Wi1472/5). We thank Dr Carsten Korth for providing N2a cells. We are grateful to Olga Dietz for technical support in protein purification.

References

1 Macdonald RL & Olsen RW (1994) GABAA receptor channels. *Annu Rev Neurosci* **17**, 569–602.
2 Moss SJ & Smart TG (2001) Constructing inhibitory synapses. *Nat Rev Neurosci* **2**, 240–250.
3 Kneussel M (2002) Dynamic regulation of GABA(A) receptors at synaptic sites. *Brain Res Brain Res Rev* **39**, 74–83.
4 Wang H, Bedford FK, Brandon NJ, Moss SJ & Olsen RW (1999) GABA(A)-receptor-associated protein links GABA(A) receptors and the cytoskeleton. *Nature* **397**, 69–72.
5 Leil TA, Chen Z-W, Chang C-SS & Olsen RW (2004) GABAA receptor-associated protein traffics GABAA receptors to the plasma membrane in neurons. *J Neurosci* **24**, 11429–11438.
6 Chen L, Wang H, Vicini S & Olsen RW (2000) The gamma-aminobutyric acid type A GABAA) receptor-associated protein (GABARAP) promotes GABAA receptor clustering and modulates the channel kinetics. *Proc Natl Acad Sci USA* **97**, 11557–11562.
7 Luu T, Gage P & Tierney M (2006) GABA increases both the conductance and mean open time of recombinant GABAA channels co-expressed with GABARAP. *J Biol Chem* **281**, 35699–35708.
8 Tanida I, Komatsu M, Ueno T & Kominami E (2003) GATE-16 and GABARAP. Are authentic modifiers mediated by Apg7 and Apg3. *Biochem Biophys Res Commun* **300**, 637–644.
9 Sou Y-S, Tanida I, Komatsu M, Ueno T & Kominami E (2006) Phosphatidylserine in addition to phosphatidylethanolamine is an in vitro target of the mammalian Atg8 modifiers Lc3, GABARAP, and GATE-16. *J Biol Chem* **281**, 3017–3024.
10 Kittler JT, Rostaing P, Schiavo G, Fritschy JM, Olsen R, Triller A & Moss SJ (2001) The subcellular distribution of GABARAP and its ability to interact with NSF suggest a role for this protein in the intracellular transport of GABA(A) receptors. *Mol Cell Neurosci* **18**, 13–25.
11 Okazaki N, Yan J, Yuasa S, Ueno T, Kominami E, Masuho Y, Koga H & Muramatsu M (2000) Interaction of the Unc-51-like kinase and microtubule-associated protein light chain 3 related proteins in the brain: possible role of vesicular transport in axonal elongation. *Brain Res Mol Brain Res* **85**, 1–12.
12 Green F, O'Hare T, Blackwell A & Enns CA (2002) Association of human transferrin receptor with GABARAP. *FEBS Lett* **518**, 101–106.
13 Kanematsu T, Jang IS, Yamaguchi T, Nagahama H, Yoshimura K, Hidaka K, Matsuda M, Takeuchi H, Misumi Y, Nakayama K *et al.* (2002) Role of the PLC-related, catalytically inactive protein p130 in GABA(A) receptor function. *EMBO J* **21**, 1004–1011.
14 Kittler JT, Arancibia-Carcamo IL & Moss SJ (2004) Association of GRIP1 with a GABA(A) receptor associated protein suggests a role for GRIP1 at inhibitory synapses. *Biochem Pharmacol* **68**, 1649–1654.
15 Kneussel M, Haverkamp S, Fuhrmann JC, Wang H, Wassle H, Olsen RW & Betz H (2000) The gamma-aminobutyric acid type A receptor (GABAAR)-associated protein GABARAP interacts with gephyrin but is not involved in receptor anchoring at the synapse. *Proc Natl Acad Sci USA* **97**, 8594–8599.
16 Lee JH, Rho SB & Chun T (2005) GABAA receptor-associated protein (GABARAP) induces apoptosis by interacting with DEAD (Asp-Glu-Ala-Asp/His) box polypeptide 47 (DDX 47). *Biotechnol Lett* **27**, 623–628.
17 Tran T, Hoffmann S, Wiesehan K, Jonas E, Luge C, Aladag A & Willbold D (2005) Insights into human Lck SH3 domain binding specificity: different binding modes of artificial and native ligands. *Biochemistry* **44**, 15042–15052.

18 Afshar N, Black BE & Paschal BM (2005) Retrotranslocation of the chaperone calreticulin from the endoplasmic reticulum lumen to the cytosol. *Mol Cell Biol* **25**, 8844–8853.
19 Tanida I, Wakabayashi M, Kanematsu T, Minematsu-Ikeguchi N, Sou Y-S, Hirata M, Ueno T & Kominami E (2006) Lysosomal turnover of GABARAP–phospholipid conjugate is activated during differentiation of C2C12 cells to myotubes without inactivation of the mTor kinase-signaling pathway. *Autophagy* **2**, 264–271.
20 Myszka D (1997) Kinetic analysis of macromolecular interactions using surface plasmon resonance biosensors. *Curr Opin Biotechnol* **8**, 50–57.
21 Stangler T, Hartmann R, Willbold D, & Koenig BW (2006) Modern high resolution NMR for the study of structure, dynamics and interactions of biological macromolecules. *Z Phys Chem* **220**, 567–613.
22 Stangler T, Mayr LM, Dingley AJ, Luge C & Willbold D (2001) Sequence-specific 1H, 13C and 15N resonance assignments of human GABA receptor associated protein. *J Biomol NMR* **21**, 183–184.
23 Jorgensen CS, Ryder LR, Steino A, Hojrup P, Hansen J, Beyer NH, Heegaard NHH & Houen G (2003) Dimerization and oligomerization of the chaperone calreticulin. *Eur J Biochem* **270**, 4140–4148.
24 Rizvi SM, Mancino L, Thammavongsa V, Cantley RL & Raghavan M (2004) A polypeptide binding conformation of calreticulin is induced by heat shock, calcium depletion, or by deletion of the C-terminal acidic region. *Mol Cell* **15**, 913–923.
25 Ellgaard L, Riek R, Herrmann T, Guntert P, Braun D, Helenius A & Wuthrich K (2001) NMR structure of the calreticulin P-domain. *Proc Natl Acad Sci USA* **98**, 3133–3138.
26 Smothers JF & Henikoff S (2001) Predicting in vivo protein peptide interactions with random phage display. *Comb Chem High Throughput Screen* **4**, 585–591.
27 Knight D, Harris R, McAlister MSB, Phelan JP, Geddes S, Moss SJ, Driscoll PC & Keep NH (2002) The X-ray crystal structure and putative ligand-derived peptide binding properties of gamma-aminobutyric acid receptor type A receptor-associated protein. *J Biol Chem* **277**, 5556–5561.
28 Coyle JE, Qamar S, Rajashankar KR & Nikolov DB (2002) Structure of GABARAP in two conformations: implications for GABA(A) receptor localization and tubulin binding. *Neuron* **33**, 63–74.
29 Michalak M, Corbett EF, Mesaeli N, Nakamura K & Opas M (1999) Calreticulin: one protein, one gene, many functions. *Biochem J* **344**, 281–292.
30 Dedhar S (1994) Novel functions for calreticulin: interaction with integrins and modulation of gene expression? *Trends Biochem Sci* **19**, 269–271.
31 Johnson S, Michalak M, Opas M & Eggleton P (2001) The ins and outs of calreticulin: from the ER lumen to the extracellular space. *Trends Cell Biol* **11**, 122–129.
32 Rojiani MV, Finlay BB, Gray V & Dedhar S (1991) In vitro interaction of a polypeptide homologous to human Ro/SS-A antigen (calreticulin) with a highly conserved amino acid sequence in the cytoplasmic domain of integrin alpha subunits. *Biochemistry* **30**, 9859–9866.
33 Coppolino MG, Woodside MJ, Demaurex N, Grinstein S, St-Arnaud R & Dedhar S (1997) Calreticulin is essential for integrin-mediated calcium signalling and cell adhesion. *Nature* **386**, 843–847.
34 Holaska JM, Black BE, Love DC, Hanover JA, Leszyk J & Paschal BM (2001) Calreticulin is a receptor for nuclear export. *J Cell Biol* **152**, 127–140.
35 Dedhar S, Rennie PS, Shago M, Hagesteijn CY, Yang H, Filmus J, Hawley RG, Bruchovsky N, Cheng H & Matusik RJ (1994) Inhibition of nuclear hormone receptor activity by calreticulin. *Nature* **367**, 480–483.
36 Tsai B, Ye Y & Rapoport TA (2002) Retro-translocation of proteins from the endoplasmic reticulum into the cytosol. *Nat Rev Mol Cell Biol* **3**, 246–255.
37 Frickel E-M, Riek R, Jelesarov I, Helenius A, Wuthrich K & Ellgaard L (2002) TROSY–NMR reveals interaction between ERp57 and the tip of the calreticulin P-domain. *Proc Natl Acad Sci USA* **99**, 1954–1959.
38 Kapoor M, Srinivas H, Kandiah E, Gemma E, Ellgaard L, Oscarson S, Helenius A & Surolia A (2003) Interactions of substrate with calreticulin, an endoplasmic reticulum chaperone. *J Biol Chem* **278**, 6194–6200.
39 Saito Y, Ihara Y, Leach MR, Cohen-Doyle MF & Williams DB (1999) Calreticulin functions in vitro as a molecular chaperone for both glycosylated and non-glycosylated proteins. *EMBO J* **18**, 6718–6729.
40 Steino A, Jorgensen CS, Laursen I & Houen G (2004) Interaction of C1q with the receptor calreticulin requires a conformational change in C1q. *Scand J Immunol* **59**, 485–495.
41 Schrag JD, Bergeron JJ, Li Y, Borisova S, Hahn M, Thomas DY & Cygler M (2001) The structure of calnexin, an ER chaperone involved in quality control of protein folding. *Mol Cell* **8**, 633–644.
42 Kapoor M, Ellgaard L, Gopalakrishnapai J, Schirra C, Gemma E, Oscarson S, Helenius A & Surolia A (2004) Mutational analysis provides molecular insight into the carbohydrate-binding region of calreticulin: pivotal roles of tyrosine-109 and aspartate-135 in carbohydrate recognition. *Biochemistry* **43**, 97–106.
43 Clegg DO, Wingerd KL, Hikita ST & Tolhurst EC (2003 May) Integrins in the development, function and dysfunction of the nervous system. *Front Biosci* **8**, d723–d750.
44 Leung-Hagesteijn CY, Milankov K, Michalak M, Wilkins J & Dedhar S (1994) Cell attachment to extracellular matrix substrates is inhibited upon downregulation

of expression of calreticulin, an intracellular integrin alpha-subunit-binding protein. *J Cell Sci* **107**, 589–600.
45 Kawaguchi S-y & Hirano T (2006) Integrin alpha3beta1 suppresses long-term potentiation at inhibitory synapses on the cerebellar Purkinje neuron. *Mol Cell Neurosci* **31**, 416–426.
46 Kennedy TE, Kuhl D, Barzilai A, Sweatt JD & Kandel ER (1992) Long-term sensitization training in Aplysia leads to an increase in calreticulin, a major presynaptic calcium-binding protein. *Neuron* **9**, 1013–1024.
47 Nakamura K, Zuppini A, Arnaudeau S, Lynch J, Ahsan I, Krause R, Papp S, De Smedt H, Parys JB, Muller-Esterl W *et al*. (2001) Functional specialization of calreticulin domains. *J Cell Biol* **154**, 961–972.
48 Harada K, Takeuchi H, Oike M, Matsuda M, Kanematsu T, Yagisawa H, Nakayama K-II, Maeda K, Erneux C & Hirata M (2005) Role of PRIP-1, a novel Ins(1,4,5)P3 binding protein, in Ins(1,4,5)P3-mediated Ca2+ signaling. *J Cell Physiol* **202**, 422–433.
49 Seeler JS & Dejean A (2001) SUMO: of branched proteins and nuclear bodies. *Oncogene* **20**, 7243–7249.
50 Corbett EF, Oikawa K, Francois P, Tessier DC, Kay C, Bergeron JJ, Thomas DY, Krause KH & Michalak M (1999) Ca2+ regulation of interactions between endoplasmic reticulum chaperones. *J Biol Chem* **274**, 6203–6211.
51 Holaska JM, Black BE, Rastinejad F & Paschal BM (2002) Ca2+-dependent nuclear export mediated by calreticulin. *Mol Cell Biol* **22**, 6286–6297.
52 Thompson JD, Gibson TJ, Plewniak F, Jeanmougin F & Higgins DG (1997) The CLUSTAL_X windows interface: flexible strategies for multiple sequence alignment aided by quality analysis tools. *Nucleic Acids Res* **25**, 4876–4882.
53 Gribskov M, McLachlan AD & Eisenberg D (1987) Profile analysis: detection of distantly related proteins. *Proc Natl Acad Sci USA* **84**, 4355–4358.
54 Bailey TL & Gribskov M (1998) Combining evidence using p-values: application to sequence homology searches. *Bioinformatics* **14**, 48–54.
55 Miroux B & Walker JE (1996) Over-production of proteins in *Escherichia coli*: mutant hosts that allow synthesis of some membrane proteins and globular proteins at high levels. *J Mol Biol* **260**, 289–298.
56 Mataruga A, Kremmer E & Muller F (2007) Type 3a and type 3b OFF cone bipolar cells provide for the alternative rod pathway in the mouse retina. *J Comp Neurol* **502**, 1123–1137.
57 Delaglio F, Grzesiek S, Vuister GW, Zhu G, Pfeifer J & Bax A (1995) NMRPipe: a multidimensional spectral processing system based on UNIX pipes. *J Biomol NMR* **6**, 277–293.
58 Keller R (2004) *The Computer Aided Resonance Assignment Tutorial*. CANTINA-Verlag, Zurich.
59 Schneider TD & Stephens RM (1990) Sequence logos: a new way to display consensus sequences. *Nucleic Acids Res* **18**, 6097–6100.
60 Pieper U, Eswar N, Braberg H, Madhusudhan MS, Davis FP, Stuart AC, Mirkovic N, Rossi A, Marti-Renom MA, Fiser A *et al*. (2004) MODBASE, a database of annotated comparative protein structure models, and associated resources. *Nucleic Acids Res* **32**, D217–D222.
61 Pettersen EF, Goddard TD, Huang CC, Couch GS, Greenblatt DM, Meng EC & Ferrin TE (2004) UCSF Chimera – a visualization system for exploratory research and analysis. *J Comput Chem* **25**, 1605–1612.